Hindawi
International Journal of Aerospace Engineering
Volume 2020, Article ID 4851909, 8 pages
https://doi.org/10.1155/2020/4851909

Research Article

FDA-MIMO Beampattern Synthesis with Hamming Window Weighted Linear Frequency Increments

Ming Tan,[1] **Chunyang Wang**,[1] **Hui Yuan**,[1] **Juan Bai**,[1] **and Lei An**[2]

[1]*Air and Missile Defense College, Air Force Engineering University, Xi'an, Shanxi 710051, China*
[2]*Aeronautics Engineering College, Air Force Engineering University, Xi'an, Shanxi 710051, China*

Correspondence should be addressed to Ming Tan; tanming_1992@163.com

Received 27 November 2019; Revised 9 February 2020; Accepted 20 March 2020; Published 16 April 2020

Academic Editor: Ennes Sarradj

By utilizing a tiny frequency increment across the array elements, frequency diverse array (FDA) generates a beampattern possessing the property of range-angle-dependent. However, the beampattern of the conventional FDA is "S"-shaped, which means it is coupled in range-angle domains, resulting in low target indication accuracy and poor jamming suppression ability. In this paper, taking advantage of multiple-input multiple-output (MIMO) technique and multiple matched filters, a new FDA framework using Hamming window weighted linear frequency increments is proposed. Correct FDA-MIMO framework and multiple matched filters are used to remove the influence of the time parameter. A range-angle-decoupled beampattern with sharp pencil-shaped mainlobe and low sidelobe levels can be produced. Comparing with the existing FDA-decoupled transmit beampattern design methods, a more focusing beampattern can be achieved. Simulation results validate the superiority of the proposed system.

1. Introduction

Phased array (PA) has been widely applied because it can electronically scan to desired direction with high directional gains [1]. Given that the beam steering of phased array shares the same gain over all the range cells at a fixed angle, it is hard for phased array to deal with range-dependent target indication as well as range-dependent interference suppression. To address the current need for more degrees of freedom, a flexible array called frequency diverse array (FDA) is proposed [2]. By applying a tiny frequency offset across the array elements, the FDA generates a transmit beampattern which is range-angle-dependent and time-variant [3]. It gives more degrees of freedom in the range dimension [4].

Owing to its ability of range-angle-dependent, the FDA has exceptional application potential in radar and navigation [5–7]. Many studies about FDA have been presented in recent years [8–17]. Many researchers take their exploration in getting rid of the disadvantages of FDA beampattern such as range-angle coupling [18–20] and time-variant [21, 22]. Taking use of the range-angle property, many methods are proposed for the FDA in range-angle two-dimensional localization [23, 24] and mainlobe deceptive jamming suppression [25, 26]. Furthermore, the FDA is utilized in combination with advanced radar systems such as multiple-input multiple-output (MIMO) radar [27, 28] and cognitive radar [29, 30] for performance improvement. In [18], a new FDA scheme with logarithmically increasing frequency offset is proposed, and the target can be located at a single maximum. A uniformly spaced symmetric FDA with nonuniform frequency offsets is proposed to form a range-angle-decoupled beampattern [19]. By employing particle swarm optimization algorithm to optimally determine the frequency offsets and element spacing, a pencil beampattern design approach is proposed, which also has lower sidelobes in range-angle dimensions [20]. To achieve a time-invariant beampattern, an approach for the FDA which uses time-dependent frequency offset (TDFO) is presented [21]. In [22], a FDA scheme using time-modulated optimized frequency offset (TMOFO) is proposed to realize time-invariant spatial fine focusing beampatterns. For target range-angle localization, a localization system which combines subarray-based FDA

and full-band FDA is proposed [23]. In [24], a method for FDA localization using a two-stage estimator is presented, and the localization performance is analyzed and discussed. Taking advantage of the FDA-MIMO radar, a subspace projection-based sample selection method is proposed to alleviate the mainlobe deceptive jamming suppression problem [25]. An approach utilizing nonhomogeneous sample detection in FDA-MIMO is proposed to suppress the deceptive jamming in the mainlobe [26]. Combining FDA with MIMO, the performance of joint range, angle, and Doppler estimation is analyzed [27]. Based on FDA-MIMO, the Cramér-Rao lower bound (CRLB) and mean square error (MSE) expressions are derived [28]. By exploiting the strengths of cognitive radar with situational awareness and FDA with range-angle-dependent beampattern, a cognitive FDA radar with situational awareness is proposed [29]. A cognitive transmit beamforming scheme which uses FDA-MIMO is presented to enhance the low probability of intercept (LPI) capability [30]. For joint radar and communication applications, a range-angle-dependent beampattern design method which adopts FDA with null depth control is proposed [31].

According to the analysis in [32, 33], most of the methods about the beampattern of FDA do not take the signal propagation delay and time-range relationship into consideration. The consideration about time-range relationship is essential [33], and the study in [32] did make an outstanding contribution in the correction of time-range relationship and frequency-phase relationship. However, after our newly derivation about FDA in [17], we find that the correction in [32] is important but not comprehensive. The signal model cannot be corrected just dependent on subtracting the delay caused by propagation distance from time, and the range-angle-dependent transmit beampattern is unconvincing for the FDA radar, leading to the invalidity of the existing range-angle-decoupled beampattern design methods. Furthermore, we also find that the method which is presented in [34, 35] is an effective measure to eliminate the time parameter in the transmit-receive beampattern. The key point of the elimination is the adoption of a series of mixers and matched filters at a receiver. Similarly, the employment of FDA-MIMO radar and multiple matched filters at the receiver also can produce a beampattern without the influence of time parameter [25, 26]. Besides, the transmit beampattern is supposed to be the equivalent transmit beampattern at the receiver, which is range-angle-dependent and time-invariant.

In this paper, based on MIMO and multiple matched filter technologies, a new FDA scheme with Hamming window weighted linear frequency increments is proposed. Different from the existing method of FDA using Hamming window-based frequency offsets whose beampattern is time-variant and symmetrical, our proposed scheme gives a solution for the problem of time variance and provides a decoupled range-angle-dependent beampattern with a narrow mainlobe and low sidelobe level. Comparing with the existing FDA systems, the superiority in beampattern performance of the proposed scheme is analyzed.

The remainder of this paper is organized as follows. Section 2 introduces the theoretical analysis about the proposed framework using FDA-MIMO. The beampattern design approach and the condition for equal comparison with other existing design methods are presented in Section 3. Numerical results and discussions are shown in Section 4. Finally, conclusions are drawn in Section 5.

2. Theoretical Analysis

According to [32], the array factor of pulse FDA should be expressed as (refer to Table I in [32])

$$\begin{aligned}\mathrm{AF} &= \mathrm{rect}\left(\frac{t-r_n/c}{T_\mathrm{p}}\right) e^{j2\pi f_0(t-(r_0/c))} \sum_{n=0}^{N-1} e^{j2\pi[f_0(nd\,\sin\theta/c)+n\Delta f(t-(r_n/c))]} \\ &= \mathrm{rect}\left(\frac{t-r_n/c}{T_\mathrm{p}}\right) \sum_{n=0}^{N-1} e^{j2\pi[f_0(t-(r_n/c))+n\Delta f(t-(r_n/c))]},\end{aligned} \tag{1}$$

where T_p is the pulse duration, c is the speed of light, r_n denotes the distance between the target and the nth element, f_0 represents the carrier frequency, d is the interelement spacing, and Δf is the frequency offset unit. Note that according to (1), the term $\mathrm{rect}[(t-r_n/c)/T_\mathrm{p}]$ $e^{j2\pi[f_0(t-(r_n/c))+n\Delta f(t-(r_n/c))]}$ is limited by $t \in [r_n/c, r_n/c+T_\mathrm{p}]$. The phase difference between each element and reference element (such as $\mathrm{rect}[(t-r_n/c)/T_\mathrm{p}]e^{j2\pi[f_0(t-(r_n/c))+n\Delta f(t-(r_n/c))]}$ and $\mathrm{rect}[(t-r_0/c)/T_\mathrm{p}]e^{j2\pi[f_0(t-(r_0/c))]}$) becomes 0. Imagine the principle of phased array, i.e., $\Delta f = 0$; the array factor (1) becomes

$$\mathrm{AF} = \sum_{n=0}^{N-1} \mathrm{rect}\left(\frac{t-r_n/c}{T_\mathrm{p}}\right) e^{j2\pi[f_0(t-(r_n/c))]}. \tag{2}$$

Also, the phase difference between each element and reference element (such as $\mathrm{rect}[(t-r_n/c)/T_\mathrm{p}]e^{j2\pi[f_0(t-(r_n/c))]}$ and $\mathrm{rect}[(t-r_0/c)/T_\mathrm{p}]e^{j2\pi[f_0(t-(r_0/c))]}$) becomes 0, which means that the array factor of phased array is not associated with the angle parameter, resulting in angle-independent property for phased array. Obviously, it is not consistent with the working principle of phased array radar. So, we made reanalysis about the basic signal model of FDA; a more detailed analysis is reflected in [17]. After our correction, the array factor of pulse FDA can be expressed as

$$\begin{aligned}\mathrm{AF}^{\mathrm{FDA}} = \mathrm{rect}&\left(\frac{t-r_0/c}{T_\mathrm{p}}\right) e^{j2\pi f_0(t-(r_0/c))} \\ &\cdot \sum_{n=0}^{N-1} e^{j2\pi n[f_0(d\,\sin\theta/c)+\Delta f(t-r_0/c)]}.\end{aligned} \tag{3}$$

Note that in (3), $t - r_0/c = t'$ is the time index within radar pulse which is limited to $t' \in [0, T_p]$, and the actual time t contains the transmit delay τ and the time index within radar pulse t', i.e., $t = \tau + t'$. This is the exact understanding

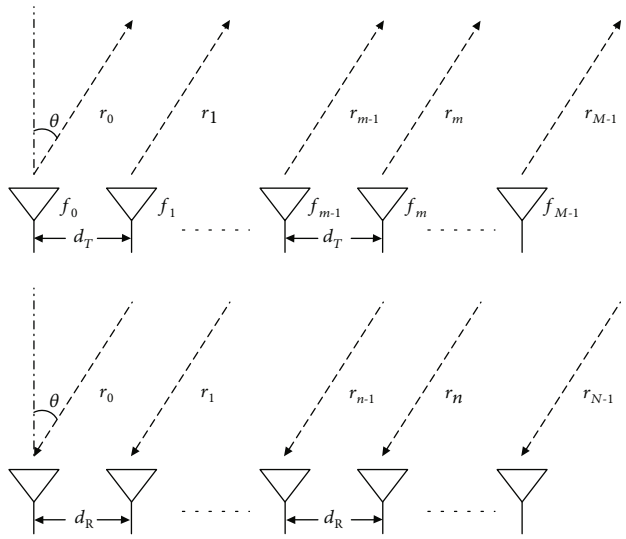

Figure 1: Configuration of FDA-MIMO.

about time-range relationship. When it comes to phased array, the array factor can be rewritten as

$$\mathrm{AF}^{\mathrm{PA}} = \mathrm{rect}\left(\frac{t - r_0/c}{T_{\mathrm{p}}}\right) e^{j2\pi f_0(t-(r_0/c))} \sum_{n=0}^{N-1} e^{j2\pi n f_0 (d \sin\theta/c)}. \quad (4)$$

Then, the phase difference becomes $2\pi n f_0 d \sin\theta/c$ associated with the parameter of angle, which is consistent with the theory of phased array radar. In the sequel, we find that there is a misconception in the original signal model of FDA, so the correction in [32] is important but not comprehensive because the original signal model of FDA needs to be corrected rather than the scope of time only and multiple matched filters at the receiver should be adopted to create and utilize the available range-dependent property of FDA.

We consider a MIMO radar; the transmit arrays and the receive arrays are both uniform linear arrays. The numbers of transmit array elements and receive array elements are M and N, respectively. The carrier frequency is f_0, and the transmit interelement spacing d_{T} and receive interelement spacing d_{R} are both half wavelength. The configuration of FDA-MIMO is shown in Figure 1.

Taking the first element as the reference element, the transmitting signal of the mth element can be expressed as

$$s_m(t) = \varphi_m(t) \exp\{j2\pi(f_0 + \Delta f_m)t\}, \quad (5)$$

where Δf_m is the frequency offset corresponding to the m th element and $\varphi_m(t)$ is the basement orthogonal modulation wave of the mth element which is supposed to be satisfied with

$$\int \varphi_{m1}{}^*(t) \cdot \varphi_{m2}(t-\tau) e^{j2\pi(\Delta f_{m1} - \Delta f_{m2})t} dt = 0, \quad m1 \neq m2, \forall\tau, \quad (6)$$

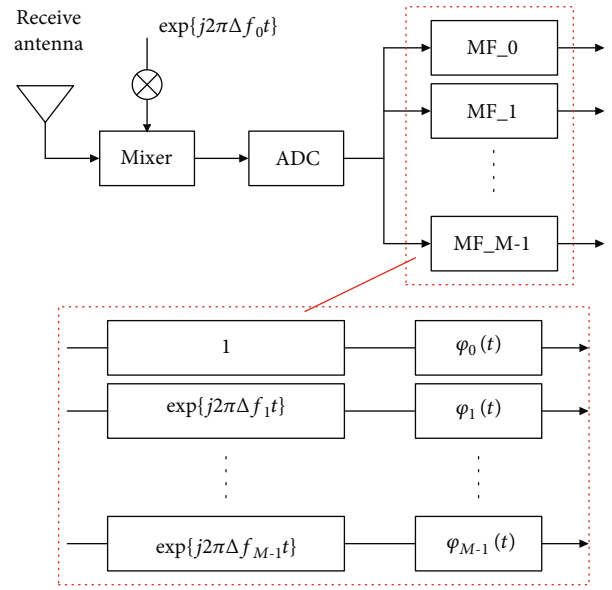

Figure 2: Matched filtering signal processing at the receiver.

where * is the conjugate operation. Hence, for a far-field target is located at range r and angle θ. According to the correction analysis of FDA about time in [17] and the FDA-MIMO radar framework in [25], the receiving signal of the nth element from the mth transmit array element can be written as

$$x_{r,m,n}(t - 2r/c) = \xi_r \varphi_m(t) \exp\{j2\pi(f_0 + \Delta f_m)(t - \tau_{m,n})\}, \quad (7)$$

where ξ_r is the complex coefficient of the signal, $\tau_{m,n}$ is the time delay from the mth transmit array element to the nth receive element, and it can be given by

$$\tau_{m,n} = \tau_0 - d_{\mathrm{T}} m \sin\theta/c - d_{\mathrm{R}} n \sin\theta/c, \quad (8)$$

where $\tau_0 = 2r/c$ is the reference time delay with respect to the reference elements of transmit and receive. Note that $t - 2r/c = t'$ is the time index within radar pulse which is limited to $t' \in [0, T_{\mathrm{p}}]$. Then, the receiving signal of the nth receive element can be expressed as

$$x_{r,n}(t) = \sum_{m=0}^{M-1} \xi_r \varphi_m(t) \exp\{j2\pi(f_0 + \Delta f_m) \cdot (t - \tau_0 + d_{\mathrm{T}} m \sin\theta/c + d_{\mathrm{R}} n \sin\theta/c)\}. \quad (9)$$

In the signal processing chain at the receiver, the received signal is mixed with $e^{j2\pi f_0 t}$ in an analogue device, then mixed with $e^{j2\pi\Delta f_m t}$ in a digital device, and matched filtered with $\varphi_m(t)$ also in a digital device, as shown in Figure 2. So after matched filtering, the signal becomes

$$x_{s,n} \approx \xi_s \sum_{m=0}^{M-1} \exp\{j2\pi[f_0(d_T m \sin\theta/c + d_R n \sin\theta/c) - \Delta f_m(2r/c)]\}, \quad (10)$$

where ξ_s is the complex coefficient after matched filtering. In the sequel, the total signal is given by

$$S \approx \xi_s \mathbf{a}(r,\theta) \otimes \mathbf{b}(\theta), \quad (11)$$

where $\mathbf{a}(r,\theta)$ and $\mathbf{b}(\theta)$ are, respectively, the transmit and receive steering vectors, and they are shown as

$$\mathbf{a}(r,\theta) = \left[1, e^{j2\pi[f_0(d_T \sin\theta/c) - \Delta f_1(2r/c)]}, \cdots, e^{j2\pi[f_0(d_T(M-1) \sin\theta/c) - \Delta f_{M-1}(2r/c)]}\right]^T,$$
$$\mathbf{b}(\theta) = \left[1, e^{j2\pi f_0 d_R \sin\theta/c}, \cdots, e^{j2\pi f_0 d_R(N-1) \sin\theta/c}\right]^T, \quad (12)$$

where $[\cdot]^T$ denotes the transpose operation. Thus, the influence of the parameter of time can be removed after the signal processing at the receiver in this FDA-MIMO system. It can be observed from (11) that the range and angle information are both included in the transmit steering vector of FDA-MIMO, while the receive steering vector is only angle-dependent just like the phased array. If $\Delta f_m = 0$, the FDA-MIMO system is simplified to a conventional MIMO system.

3. Beampattern Design

The frequency offsets of the conventional FDA is linearly progressively increasing across the elements, which can be expressed as

$$\Delta f_m^{\text{Con}} = m\Delta f, \quad (13)$$

where Δf is the frequency increment unit. The transmit beampattern of the conventional FDA is range-angle coupling, and there is periodicity in the range dimension. Therefore, it will produce many peaks at the same time, which causes difficulties in range-angle localization and jamming suppression. To create a decoupled dot-shaped beampattern in range-angle dimensions, the FDA frameworks using logarithmically increasing frequency offset and Hamming window-based frequency offset are proposed in [18, 19], respectively. Whether the frequency offsets of these methods are symmetric or not, the essence of both of them is that the nonlinear frequency offset can result in an unusual beampattern which we can make full use of. The frequency offset of the log-FDA [18] can be expressed as

$$\Delta f_m^{\text{Log}} = \delta \cdot \log(m+1), \quad (14)$$

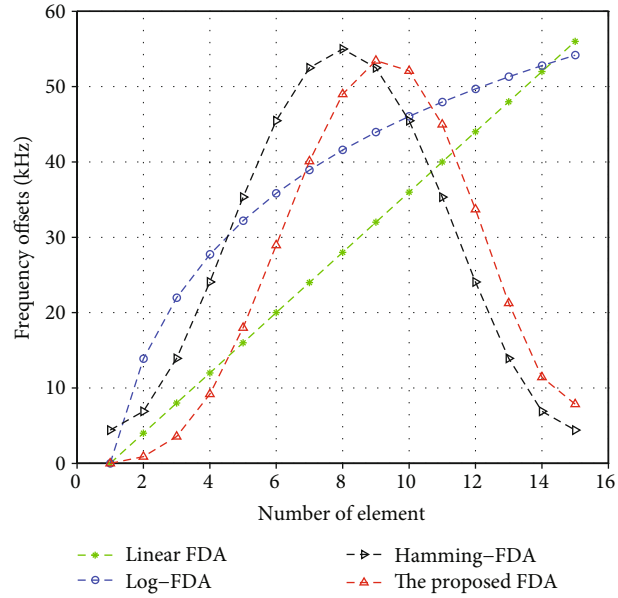

Figure 3: Frequency offset comparison.

where δ is constant. The frequency offset of the Hamming-FDA [19] can be expressed as

$$\Delta f_m^{\text{Ham}} = B\left\{0.54 - 0.46\cos\left[\frac{2\pi(m-(M+1)/2)}{M}\right]\right\}, \quad (15)$$

where B is the bandwidth and the number of elements M should be odd. In fact, due to the time-variant problem and time-range relationship for FDA in the transmit beampattern concluded in [17, 32, 33], it is impossible to form a useful range-angle-decoupled transmit beampattern just using the nonlinear frequency offset design approaches such as those in [18, 19]. Therefore, the same FDA-MIMO framework and matched filtering technique are also adopted when analyzing the transmit beampattern of log-FDA and Hamming-FDA to avoid the time-variant problem. It is noteworthy that the transmit beampatterns are the equivalent transmit beampatterns at the receiver. Besides, the performances of their beampatterns are equal with the corresponding transmit beampatterns at an instantaneous time analyzed in [18, 19]. The proposed FDA scheme in our work is with Hamming window weighted linear frequency increments, which can be expressed as

$$\Delta f_m = m\Delta f\left\{0.54 - 0.46\cos\left[\frac{2\pi(m-(M+1)/2)}{M}\right]\right\}. \quad (16)$$

It is an improved form based on the Hamming window type, and the performance will be analyzed in the following section comparing with the existing techniques. Furthermore, it outperforms the log-FDA and Hamming-FDA in terms of half-power beam width of mainlobe and sidelobe suppression.

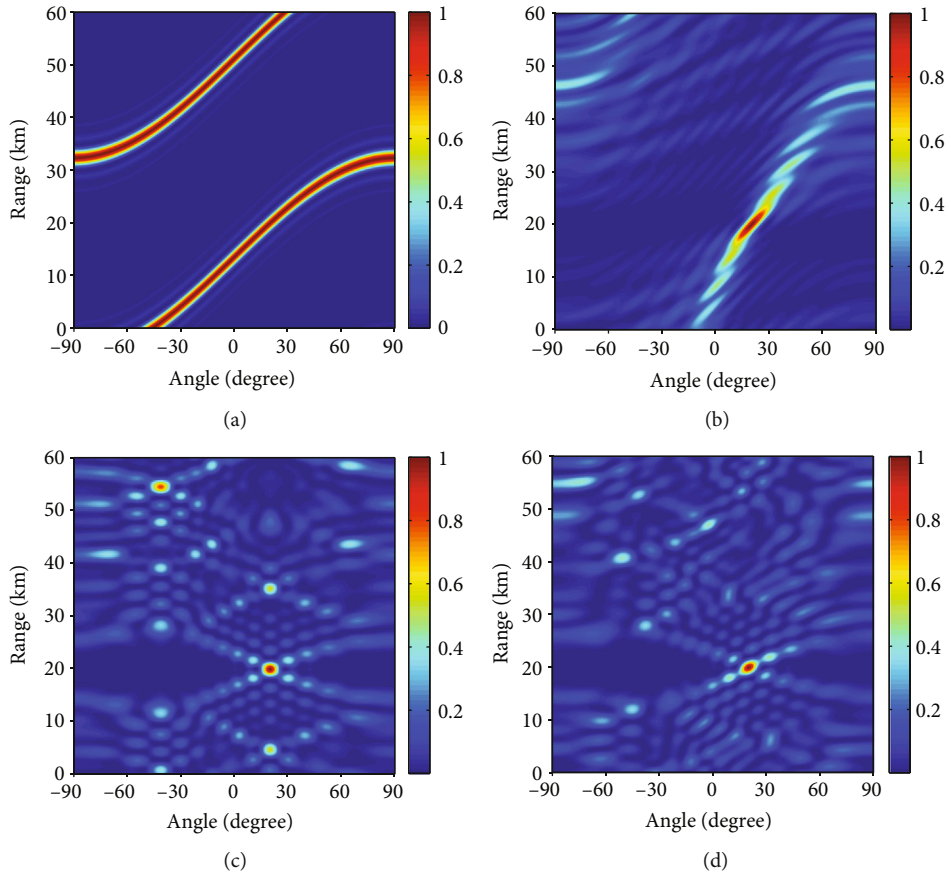

FIGURE 4: The equivalent transmit beampatterns at the receiver of (a) conventional linear FDA, (b) log-FDA, (c) Hamming-FDA, and (d) the proposed FDA.

To detect the target located at range r_0 and angle θ_0, the steering vector can be expressed as

$$w = \mathbf{a}(r,\theta) \otimes \mathbf{b}(\theta)|_{r=r_0,\theta=\theta_0}. \tag{17}$$

Consequently, the transmit-receive beampattern can be expressed as

$$B_{\mathrm{T,R}} = \left| \sum_{m=0}^{M-1} \exp\left\{ j2\pi \left(f_0 d_{\mathrm{T}} m \frac{\sin\theta - \sin\theta_0}{c} - 2\Delta f_m \frac{r - r_0}{c} \right) \right\} \right|^2 \times \left| \sum_{n=0}^{N-1} \exp\left\{ j2\pi f_0 d_R n \frac{\sin\theta - \sin\theta_0}{c} \right\} \right|^2. \tag{18}$$

Thus, the equivalent transmit beampattern at the receiver can be written as

$$B_{\mathrm{T}} = \left| \sum_{m=0}^{M-1} \exp\left\{ j2\pi \left(f_0 d_{\mathrm{T}} m \frac{\sin\theta - \sin\theta_0}{c} - 2\Delta f_m \frac{r - r_0}{c} \right) \right\} \right|^2. \tag{19}$$

So it is obviously observed that the transmit beampattern is range-angle-dependent and not associated with the parameter of time. In addition, the receive beampattern is given by

$$B_{\mathrm{R}} = \left| \sum_{n=0}^{N-1} \exp\left\{ j2\pi f_0 d_{\mathrm{R}} n \frac{\sin\theta - \sin\theta_0}{c} \right\} \right|^2. \tag{20}$$

From (21), it is seen that the receive beampattern is only angle-dependent just like the phased array.

Given the above, our proposed scheme can be termed as the FDA-MIMO with Hamming window weighted linear frequency increments. Due to the fact that there is only one carrier frequency at each element, which is similar with the log-FDA and Hamming-FDA, the complexity of the proposed FDA approach is equal with the previous nonlinear frequency offset approaches.

4. Numerical Results and Discussions

The frequency offsets of conventional linear FDA, log-FDA, Hamming-FDA, and our proposed FDA are compared as shown in Figure 3. To eliminate the unfairness, the bandwidths of these methods are approximately equal. The carrier frequency is $f_0 = 10$ GHz. The element numbers of transmit and receive are $M = N = 15$.

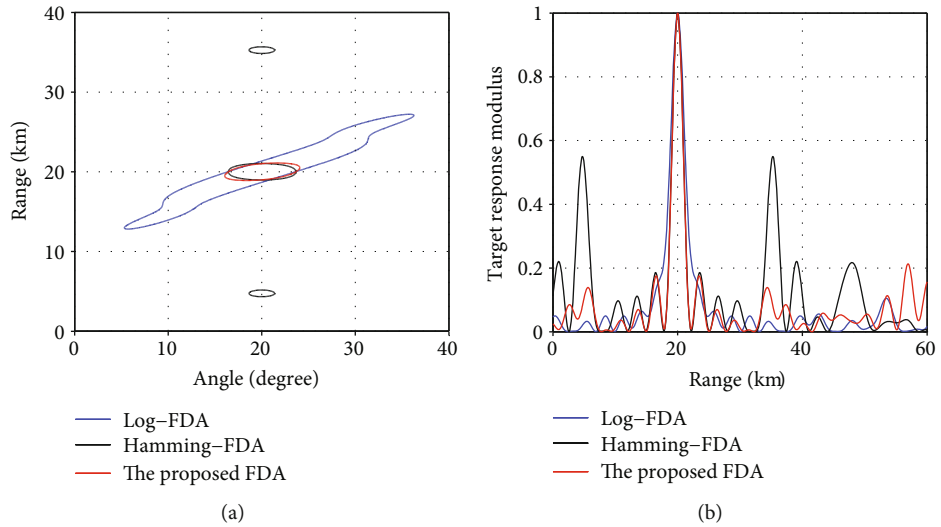

Figure 5: Comparative results of (a) half-power beam width of transmit beampatterns; (b) transmit beampatterns in the profile of range.

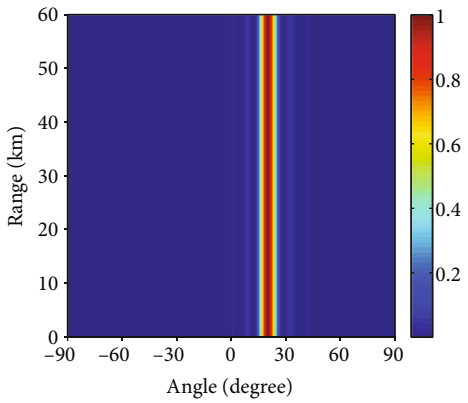

Figure 6: Receive beampattern.

For a target located at 20 km, 20°, the equivalent transmit beampatterns at the receiver after utilizing multiple matched filtering technique on the basis of the four FDA systems above are given in Figure 4. Figure 4(a) shows that the beampattern of the conventional FDA is coupled in range-angle dimensions, which is unfavorable for energy concentration. The other three approaches generate beampatterns with one single peak at the position of the target, facilitating the target localization and jamming suppression.

Figure 5(a) shows the comparative results of the half-power beam width of transmit beampatterns for the log-FDA, Hamming-FDA, and proposed FDA. Note that proposed FDA performs closely with the Hamming-FDA in terms of the beam width, and they both have better performance than the log-FDA. Nevertheless, the drawback of the Hamming-FDA is that its beampattern has high sidelobe points. To make it worse, the sidelobes appear at the same angle of the target, which is a disadvantage for range-dependent interference suppressing. When it comes to the profile of range, as plotted in Figure 5(b), the beampattern of the Hamming-FDA owns higher sidelobe levels, whereas the undesired range bins of the other two methods keep on a low level. It also can be observed from Figure 5(b) that the range resolution of the proposed scheme is better than that of the log-FDA. Therefore, the proposed FDA outperforms the log-FDA and Hamming-FDA in terms of the mainlobe beam width and the sidelobe levels.

It is noteworthy that the range-dependent property of FDA cannot be easily implemented so that the transmit-receive beampattern is more practical to take advantage of. According to the analysis aforementioned, the receive beampattern is range-independent just like the phased array, as shown in Figure 6. It can reinforce the energy of the desired angle. Meanwhile, the received signal from the uninterested directions can be weakened.

Taking advantage of the MIMO technique, the transmit-receive beampatterns of these three kinds of FDA are shown in Figure 7. It can be seen from Figure 7 that these three methods can generate a range-angle-decoupled beampattern. Comparing with the two previous approaches, our proposed scheme produces a more focusing beampattern which has a narrower mainlobe and well-performed sidelobe level. The comparison results of half-power beam width are also presented to demonstrate the outperformance of our proposed scheme over other two methods in range-angle occupied areas, as shown in Figure 8.

To sum up, using the appropriate FDA-MIMO system with multiple matched filters, the range-dependent property can be fully applied without the influence of time parameter. Moreover, the proposed FDA framework outperforms the log-FDA and Hamming-FDA in terms of half-power beam width of mainlobe and sidelobe suppression. As a result, it has better detection precision for the target, as well as a stronger jamming suppression ability for mainlobe jamming from the same angle but different range with the desired position. In addition, the property of range-angle-dependent makes it easy to steer a target in range-angle domains.

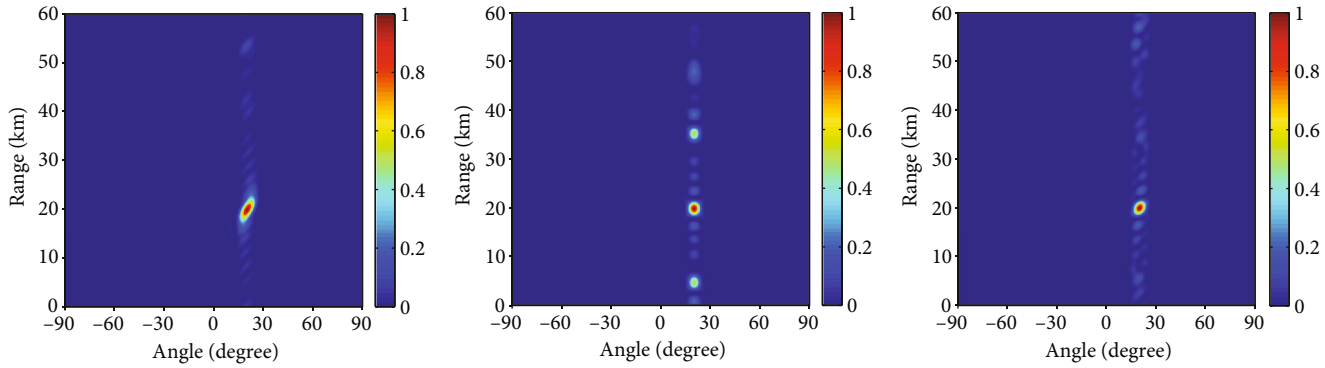

Figure 7: Transmit-receive beampatterns using MIMO radar with (a) the log-FDA, (b) the Hamming-FDA, and (c) the proposed FDA.

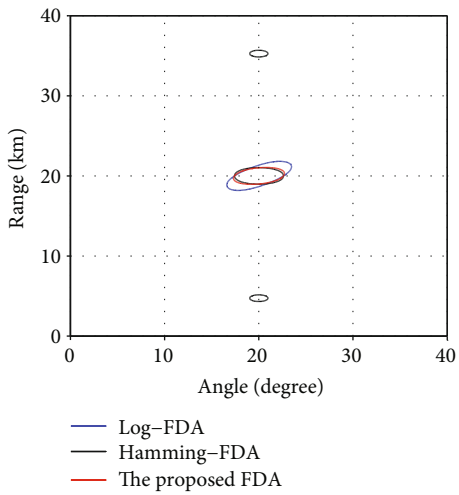

Figure 8: Half-power beam width comparison for the transmit-receive beampatterns.

5. Conclusions

In this paper, taking advantage of the MIMO technique and multiple matched filters at the receiver, the range-dependent property of the FDA radar can be fully utilized without the influence of time parameter. Furthermore, by utilizing a nonuniform frequency offset, a new FDA framework is established. The frequency offset is Hamming window weighted linearly increasing, and the array elements are uniform linearly spacing. The proposed system can generate a sharp pencil-shaped beampattern with a low sidelobe level in the range profile, which facilitates the application of target indication and jamming suppression in the aspect of range. In addition, comparing with the existing FDA in the equivalent transmit beampattern at the receiver and transmit-receive beampattern, the proposed scheme has better performance with respect to the mainlobe beam width and sidelobe levels.

Data Availability

The data used to support the findings of this study are available from the corresponding author upon request.

Conflicts of Interest

The authors declare that there are no conflicts of interest regarding the publication of this paper.

Acknowledgments

This work was supported in part by the National Natural Science Foundation of China under Grant 61601502 and 61601503 and the China Postdoctoral Science Foundation under Grant 2019M662257.

References

[1] Y. Liang, K. Zhao, Y. Chen, L. Zhang, and G. J. Bennett, "An experimental characterization on the acoustic performance of forward/rearward retraction of a nose landing gear," *International Journal of Aerospace Engineering*, vol. 2019, Article ID 4135094, 11 pages, 2019.

[2] P. Antonik, M. C. Wicks, H. D. Griffiths, and C. J. Baker, "Frequency diverse array radars," in *2006 IEEE Conference on Radar*, pp. 215–217, Verona, NY, USA, April 2006.

[3] M. Secmen, S. Demir, A. Hizal, and T. Eker, "Frequency diverse array antenna with periodic time modulated pattern in range and angle," in *2007 IEEE Radar Conference*, pp. 427–430, Boston, MA, USA, April 2007.

[4] J. Huang, K.-F. Tong, and C. J. Baker, "Frequency diverse array with beam scanning feature," in *2008 IEEE Antennas and Propagation Society International Symposium*, pp. 1–4, San Diego, CA, USA, July 2008.

[5] W.-Q. Wang, "Overview of frequency diverse array in radar and navigation applications," *IET Radar, Sonar & Navigation*, vol. 10, no. 6, pp. 1001–1012, 2016.

[6] W.-Q. Wang, "Frequency diverse array antenna: new opportunities," *IEEE Antennas and Propagation Magazine*, vol. 57, no. 2, pp. 145–152, 2015.

[7] J. Xu, S. Zhu, G. Liao, and Y. Zhang, "An overview of frequency diverse array radar technology," *Journal of Radars*, vol. 7, no. 2, pp. 167–182, 2018.

[8] J. Xu, G. Liao, S. Zhu, L. Huang, and H. C. So, "Joint range and angle estimation using MIMO radar with frequency diverse array," *IEEE Transactions on Signal Processing*, vol. 63, no. 13, pp. 3396–3410, 2015.

[9] W.-Q. Wang and H. Shao, "Range-angle localization of targets by a double-pulse frequency diverse array radar," *IEEE Journal*

of Selected Topics in Signal Processing, vol. 8, no. 1, pp. 106–114, 2014.

[10] T. Eker, S. Demir, and A. Hizal, "Exploitation of linear frequency modulated continuous waveform (LFMCW) for frequency diverse arrays," *IEEE Transactions on Antennas and Propagation*, vol. 61, no. 7, pp. 3546–3553, 2013.

[11] M. Tan, C. Wang, Z. Li, X. Li, and L. Bao, "Stepped frequency pulse frequency diverse array radar for target localization in angle and range domains," *International Journal of Antennas and Propagation*, vol. 2018, Article ID 8962048, 12 pages, 2018.

[12] J. Xu, S. Zhu, and G. Liao, "Space-time-range adaptive processing for airborne radar systems," *IEEE Sensors Journal*, vol. 15, no. 3, pp. 1602–1610, 2015.

[13] K. Wan, W.-Q. Wang, H. Chen, and S. Zhang, "Space-time modulated wideband array antenna," *IEEE Antennas and Wireless Propagation Letters*, vol. 18, no. 6, pp. 1081–1085, 2019.

[14] J. Xu, G. Liao, Y. Zhang, H. Ji, and L. Huang, "An adaptive range-angle-Doppler processing approach for FDA-MIMO radar using three-dimensional localization," *IEEE Journal of Selected Topics in Signal Processing*, vol. 11, no. 2, pp. 309–320, 2017.

[15] H. Chen, W.-Q. Wang, Y.-S. Cui, and Y. Liao, "Statistical analysis for time modulation-based frequency diverse array beampattern," *IEEE Access*, vol. 7, pp. 84142–84154, 2019.

[16] J. Xu, G. Liao, L. Huang, and H. C. So, "Robust adaptive beamforming for fast-moving target detection with FDA-STAP radar," *IEEE Transactions on Signal Processing*, vol. 65, no. 4, pp. 973–984, 2017.

[17] M. Tan, C. Wang, and Z. Li, "Correction analysis of frequency diverse array radar about time," *IEEE Transactions on Antennas and Propagation*, vol. AP1909-1910, under review.

[18] W. Khan, I. M. Qureshi, and S. Saeed, "Frequency diverse array radar with logarithmically increasing frequency offset," *IEEE Antennas and Wireless Propagation Letters*, vol. 14, pp. 499–502, 2015.

[19] A. Basit, I. M. Qureshi, W. Khan, S. . Rehman, and M. M. Khan, "Beam pattern synthesis for an FDA radar with Hamming window-based nonuniform frequency offset," *IEEE Antennas and Wireless Propagation Letters*, vol. 16, pp. 2283–2286, 2017.

[20] L. Lan, G. Liao, J. Xu, and J. Wen, "Range-angle pencil-beamforming for non-uniformly distributed array radar," *Multidimensional Systems and Signal Processing*, vol. 29, no. 3, pp. 867–886, 2018.

[21] W. Khan and I. M. Qureshi, "Frequency diverse array radar with time-dependent frequency offset," *IEEE Antennas and Wireless Propagation Letters*, vol. 13, pp. 758–761, 2014.

[22] A.-M. Yao, W. Wu, and D.-G. Fang, "Frequency diverse array antenna using time-modulated optimized frequency offset to obtain time-invariant spatial fine focusing beampattern," *IEEE Transactions on Antennas and Propagation*, vol. 64, no. 10, pp. 4434–4446, 2016.

[23] S. L. Wang, Z.-H. Xu, X. Liu, W. Dong, and G. Wang, "Subarray-based frequency diverse array for target range-angle localization with monopulse processing," *IEEE Sensors Journal*, vol. 18, no. 14, pp. 5937–5947, 2018.

[24] C. Cui, J. Xiong, W.-Q. Wang, and W. Wu, "Localization performance analysis of FDA radar receiver with two-stage estimator," *IEEE Transactions on Aerospace and Electronic Systems*, vol. 54, no. 6, pp. 2873–2887, 2018.

[25] J. Xu, J. Kang, G. Liao, and H. C. So, "Mainlobe deceptive jammer suppression with FDA-MIMO radar," in *2018 IEEE 10th Sensor Array and Multichannel Signal Processing Workshop (SAM)*, pp. 504–508, Sheffield, UK, July 2018.

[26] L. Lan, G. Liao, J. Xu, Y. Zhang, and F. Fioranelli, "Suppression approach to main-beam deceptive jamming in FDA-MIMO radar using nonhomogeneous sample detection," *IEEE Access*, vol. 6, pp. 34582–34597, 2018.

[27] J. Xu, W. Wang, C. Cui, and R. Gui, "Joint range, angle and Doppler estimation for FDA-MIMO radar," in *2018 IEEE 10th Sensor Array and Multichannel Signal Processing Workshop (SAM)*, pp. 499–503, Sheffield, UK, July 2018.

[28] J. Xiong, W.-Q. Wang, and K. Gao, "FDA-MIMO radar range–angle estimation: CRLB, MSE, and resolution analysis," *IEEE Transactions on Aerospace and Electronic Systems*, vol. 54, no. 1, pp. 284–294, 2018.

[29] W.-Q. Wang, "Cognitive frequency diverse array radar with situational awareness," *IET Radar, Sonar & Navigation*, vol. 10, no. 2, pp. 359–369, 2016.

[30] J. Xiong, W.-Q. Wang, C. Cui, and K. Gao, "Cognitive FDA-MIMO radar for LPI transmit beamforming," *IET Radar, Sonar & Navigation*, vol. 11, no. 10, pp. 1574–1580, 2017.

[31] A. Basit, W.-Q. Wang, S. Y. Nusenu, and S. Zhang, "Range-angle-dependent beampattern synthesis with null depth control for joint radar communication," *IEEE Antennas and Wireless Propagation Letters*, vol. 18, no. 9, pp. 1741–1745, 2019.

[32] K. Chen, S. Yang, Y. Chen, and S.-W. Qu, "Accurate models of time-invariant beampatterns for frequency diverse arrays," *IEEE Transactions on Antennas and Propagation*, vol. 67, no. 5, pp. 3022–3029, 2019.

[33] B. Chen, X. Chen, Y. Huang, and J. Guan, "Transmit beampattern synthesis for the FDA radar," *IEEE Antennas and Wireless Propagation Letters*, vol. 17, no. 1, pp. 98–101, 2018.

[34] Y. Xu, X. Shi, W. Li, J. Xu, and L. Huang, "Low-sidelobe range-angle beamforming with FDA using multiple parameter optimization," *IEEE Transactions on Aerospace and Electronic Systems*, vol. 55, no. 5, pp. 2214–2225, 2019.

[35] Y. Xu and J. Xu, "Corrections to "range-angle-dependent beamforming of pulsed-frequency diverse array" [Jul 15 3262-3267]," *IEEE Transactions on Antennas and Propagation*, vol. 66, no. 11, pp. 6466–6468, 2018.